Scientific article
UDC 577.112
DOI: 10.52957/2782-1900-2025-6-3-142-154

SYNTHESIS AND STUDY OF THE BIOLOGICAL ACTIVITY OF SPIROCARBON AND ITS COMPLEXES WITH CATIONS OF TRANSITION ELEMENTS

A. A. Shubina, T. N. Orlova, V. Yu. Orlov

Anna Aleksandrovna Shubina, Student**; Tatiana Nikolaevna Orlova**, Candidate of Chemical Sciences, Associate Professor; **Vladimir Yurievich Orlov**, Doctor of Chemical Sciences, Professor
P.G. Demidov Yaroslavl State University, Sovetskaya St., 14, Yaroslavl, Russia, 150003; *annashubina100@gmail.com, orl@bio.uniyar.ac.ru, eagle0802@mail.ru*

Keywords:
spirocarbon, IR spectroscopy, electronic spectroscopy, transition metals, complexation, PASS online, molecular docking.

Abstract. *The synthesis of the ligand – spirocarbon (4,4,10,10-tetramethyl-1,3,7,9-tetraazaspiro[5.5]undecane-2,8-dione) – and its coordination compounds with transition metal cations (Co^{2+}, Cd^{2+}, La^{3+}, Cu^{2+}, Zn^{2+}, Mn^{2+}) has been conducted. The formation of the coordination compounds was confirmed by IR and UV spectroscopy. The electronic spectra of the complexes recorded a bathochromic shift of the band corresponding to the ligand along and the appearance of new absorption maxima in the long-wavelength region. According to molecular docking results, the identified biological target - α-synuclein - binds to the ligand (spirocarbon) via hydrogen bonds between the oxygen and hydrogen atoms of the amide group of 4,4,10,10-tetramethyl-1,3,7,9-tetraazaspiro[5.5]undecane-2,8-dione and the hydrogen and oxygen atoms of the amino acid residues of the protein. The dependence of the spirocarbon complexes lipophilicity on the pH of the medium was investigated.*

For citation:
Shubina A.A., Orlova T.N., Orlov V.Yu. Synthesis and study of the biological activity of spirocarbon and its complexes with cations of transition elements // *From Chemistry towards Technology Step-by-Step*. 2025. Vol. 6, Iss. 3. P. 142-154. URL: https://chemintech.ru/en/nauka/issue/6423/view

Introduction

Spirocarbon or 4,4,10,10-tetramethyl-1,3,7,9-tetraazaspiro[5.5]undecane-2,8-dione is the condensed bicyclic bis-urea of the spiro series (see Fig. 1).

Spirocarbon (Sk; **1**) was first synthesised in 1901 via the condensation of acetone and urea [1]. Later, Zigeuner et al. confirmed its spirobisprimidine structure [2]. Spirocarbon exhibits a range of unique biological properties: low toxicity (LD_{50} = 3000 mg/kg) [3], membranotropic activity [4], cytotoxicity against leukemia cell lines L1210 (mice) and CEM-T4 (human) [5]. Additionally, it affects on the physicochemical and functional properties of hemoglobin and the state of the antioxidant system

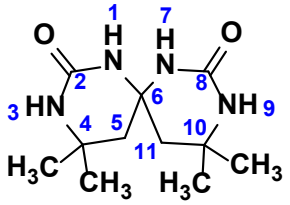

Fig. 1. Structural formula of 4,4,10,10-tetramethyl-1,3,7,9-tetraazaspiro[5.5]undecane-2,8-dione

regulating intracellular processes through NO· and its derivatives [6]. Moreover, the use of spirocarbon as a growth regulator increases protein content [7] and reduces starchiness in oat grains [8].

Indeed, Alzheimer's disease aggregates its α-synuclein form interacting with β-amyloid and enhancing its neurotoxicity [9]. α-Synuclein exacerbates oxidative stress and inflammation, disrupting synaptic transmission [10]. Acetylcholinesterase also accelerates β-amyloid aggregation, promoting the formation of toxic complexes on neuronal surfaces [11]. Therefore, acetylcholinesterase inhibitors increase acetylcholine levels, which improves signal transmission in the brain [12], and donor-acceptor groups in active pharmaceutical substances can exert antioxidant effects [13].

In study [14], spiroheterocyclic compounds, including spirocarbon, were investigated as cholinesterase inhibitors (Sk's inhibitory activity was tested using a microtiter ELISA method). Screening results demonstrated significant acetylcholinesterase inhibition potential. Thus, derivatives based on spirocarbon can be synthesised as active pharmaceutical ingredients against Alzheimer's disease. Furthermore, prospects for the application of rare-earth element complexes with spirocarbon as drug delivery agents have been proposed [15].

Therefore, spirocarbon low binding energy with α-synuclein propounds a hypothesis on spirocarbon alleviates symptoms and slows neurodegenerative processes. The synthesis of spirocarbon complexes is justified from the perspective of enhancing bioavailability compared to the unbound ligand form.

The purpose of the study is the synthesis and investigation of the spectral and biological properties of La^{3+} and *d*-element complexes with spirocarbon as an organic ligand

Experimental part

The following reagents were used for the synthesis: urea of analytical grade (AO LenReaktiv, Russia), acetone of chemical purity (AO EKOS-1, Russia), sulfuric acid of chemical purity (AO LenReaktiv, Russia), lanthanum(III) nitrate hexahydrate of chemical purity (AO LenReaktiv, Russia), and other chemically pure soluble salts of *d*-elements: copper(II) nitrate trihydrate, anhydrous zinc(II) chloride, anhydrous manganese(II) chloride, cobalt(II) nitrate hexahydrate, cadmium(II) nitrate tetrahydrate.

The absorption spectra of the synthesised products were recorded on a PE-5400 UV spectrophotometer OOO Ekroschim, St. Peterburg, Russia using ethyl alcohol as the solvent. Functional group analysis was performed by ATR-FTIR spectroscopy on a Spectrum 65 Fourier-transform IR spectrometer Perkin Elmer. We performed elemental analysis using a FLASH EA 1112 C,H,N,S analyser. The melting point of the ligand was measured on a Stuart SMO10.

Spirocarbon (4,4,10,10-tetramethyl-1,3,7,9-tetraazaspiro[5.5]undecane-2,8-dione) was synthesised according to the method [17]. The obtained compound was isolated and purified from residual impurities by recrystallisation from an aqueous solution. The melting point of spirocarbon was 241-243 ℃.

Synthesis procedure for complex compounds of spirocarbon (Sk) with soluble salts of *d*-elements and lanthanum (III) nitrate. The masses of the components are given in Table 1. A weighed sample of the corresponding salt hydrate (or anhydrous chloride) was dissolved in 20 ml of acetone and added to a solution of the ligand (Sk) in acetone. Schemes 1-6 are shown in Table 1.

Table 1. Weighed samples of substances for the synthesis of complexes

Complexing agent	Formula of the starting salt	Mass of the weighed sample of the salt, g	Mass of the weighed sample of spirocarbon, g
Cu^{2+}	$Cu(NO_3)_2{\cdot}3H_2O$	0.1330	0.2649
Zn^{2+}	$ZnCl_2$	0.1020	0.1806
Mn^{2+}	$MnCl_2$	0.1110	0.2119
Co^{2+}	$Co(NO_3)_2{\cdot}6H_2O$	0.1460	0.2408
Cd^{2+}	$Cd(NO_3)_2{\cdot}4H_2O$	0.1450	0.1132
La^{3+}	$La(NO_3)_3{\cdot}6H_2O$	0.1390	0.1541

The optimal molar ratio of substances was 1:1 for Sk complexes with Zn^{2+}, Mn^{2+}, Cd^{2+} and 1:2 for Cu^{2+}, Co^{2+}, La^{3+} (the completeness of ligand binding was verified by electronic spectroscopy). The solution was stirred for 5-15 minutes on a magnetic stirrer until a viscous solution formed. The viscous solution was filtered; the filtrate was stored in a tightly sealed vessel. After 2-3 weeks, transparent prismatic crystals are formed, filtered off, washed with acetone, and air-dried. The obtained complex compounds exhibit the best solubility in aprotic bipolar solvents. They are very soluble in DMF and DMSO, readily soluble in alcohols and acetonitrile, sparingly soluble in water, and practically insoluble in nonpolar organic solvents (hexane, etc.).

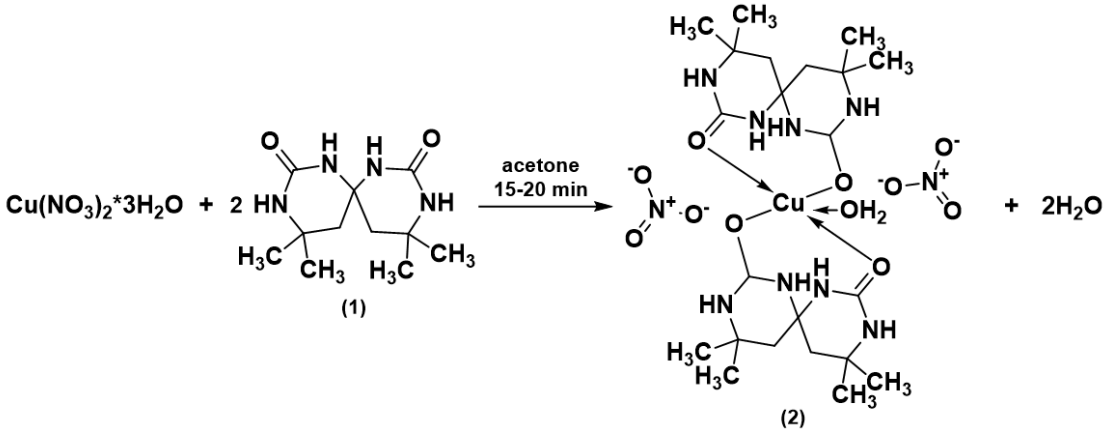

Scheme 1. Synthesis of complex **2**

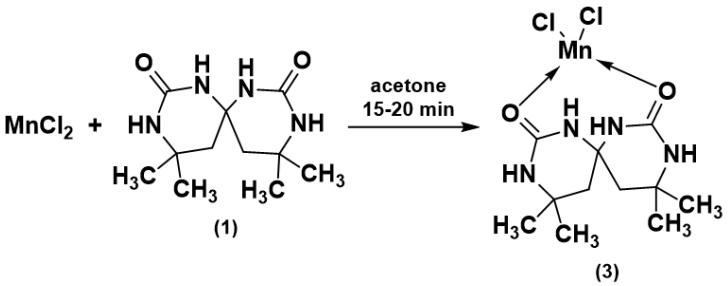

Scheme 2. Synthesis of complex **3**

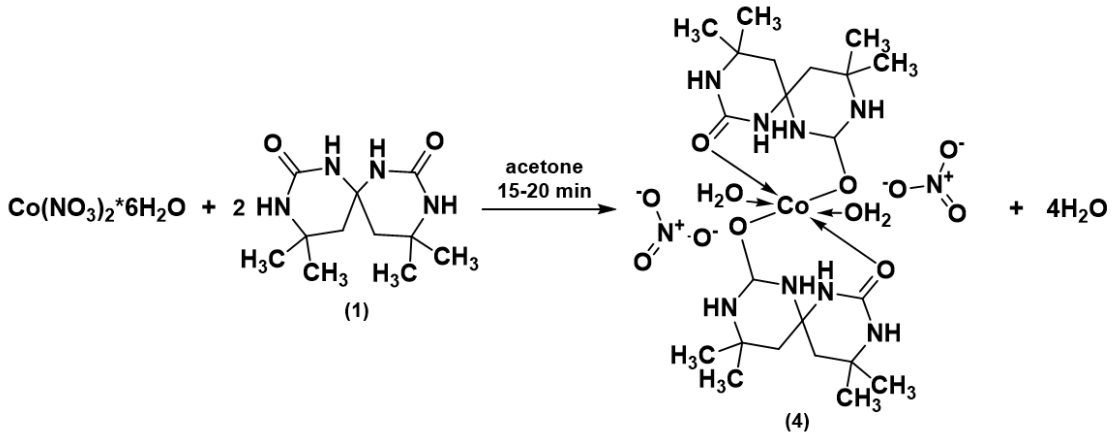

Scheme 3. Synthesis of complex **4**

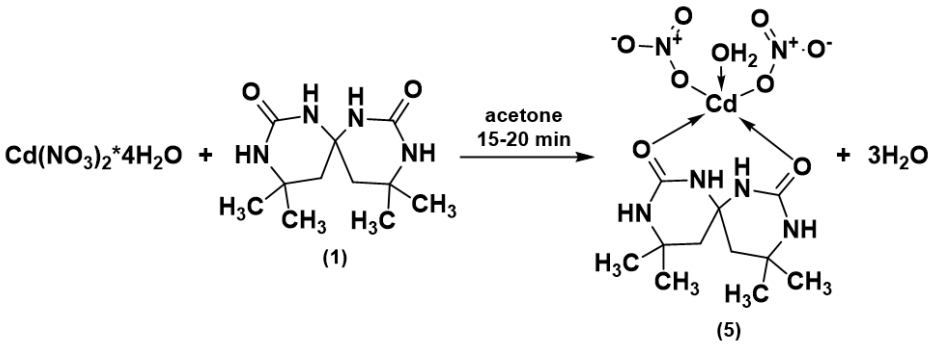

Scheme 4. Synthesis of complex **5**

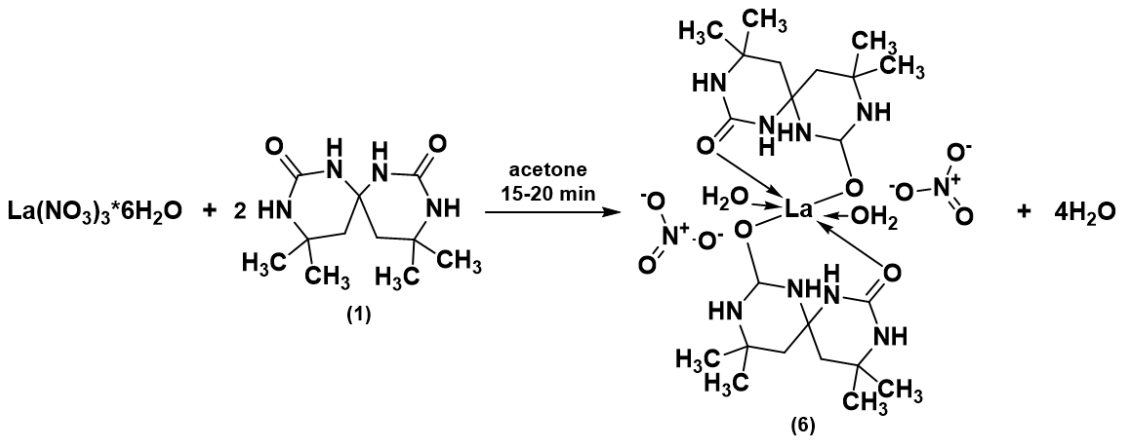

Scheme 5. Synthesis of complex **6**

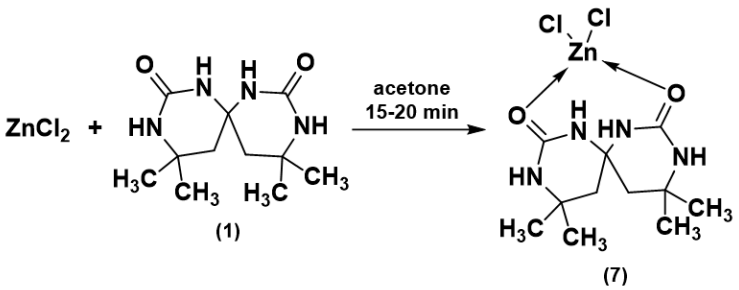

Scheme 6. Synthesis of complex **7**

Sk (**1**; ligand; gross formula $C_{11}H_{20}N_4O_2$). Yield is 96% (1.12 g). White fine-crystalline powder. Found, %: C 54.81; H 8.34; N 23.33. Calculated, %: C 54.98; H 8.39; N 23.32. IR, ν_{max}, cm^{-1}: 3310, 3295, 3203 (N-H), 3075 (CH_2), 2970, 2925 (CH_3), 1650 (C=O), 1420 (C-N). λ_{max} = 206 nm.

$[CuSk_2(H_2O)](NO_3)_2$ (**2**). Yield is 82% (0.3099 g). Pale blue crystals. Found, %: C 38.76; H 6.23; N 19.66. Calculated, %: C 38.51; H 6.17; N 19.71. IR, ν_{max}, cm^{-1}: 3630 (H_2O); 3285 (N-H); 3087, 2956, 2896 (CH_2, CH_3); 1621, 1642 (C=O, amide I); 1446 (C–N); 825 (NO_3^-). λ_{max} = 243 nm.

$[MnCl_2 \cdot Sk]$ (**3**). Yield is 87% (0.2807 g). Beige crystals. Found, %: C 37.08; H 6.51; N 20.30. Calculated, %: C 37.99; H 6.38; N 20.14. IR, ν_{max}, cm^{-1}: 3354, 3302, 3263, 3235 (N-H); 2940, 2891 (CH_3); 1645 (C=O, amide I); 1478 (C–N). λ_{max} = 269 nm.

$[CoSk_2(H_2O)_2](NO_3)_2$ (**4**). Yield is 75% (0.2560 g). Lilac crystals. Found, %: C 38.64; H 6.99; N 20.66. Calculated, %: C 38.26; H 6.28; N 20.28. IR, ν_{max}, cm^{-1}: 3650 (H_2O), 3296 (N-H), 2975, 2922, 2880 (CH_3, CH_2), 1622 (C=O, amide I), 1034, 1369, 753, 827 (NO_3^-), 1447 (C-N). λ_{max} = 515 nm.

$[Cd(NO_3)_2Sk(H_2O)]$ (**5**). Yield is 90% (0.2095 g). White crystals. Found, %: C 26.68; H 4.21; N 16.89. Calculated, %: C 26.71; H 4.48; N 16.99. IR, ν_{max}, cm^{-1}: 3570, 1501 (H_2O); 3303 (N-H); 3080 2975, 2900 (CH_2, CH_3); 1617 (C=O, amide I); 832 (NO_3^-). λ_{max} = 269 nm.

$[LaSk_2(H_2O)_2(NO_3)_3]$ (**6**). Yield is 92% (0.2530 g). Transparent prismatic crystals. Found, %: C 21.96; H 4.07; N 16.32. Calculated, %: C 21.97; H 4.02; N 16.30. IR, ν_{max}, cm^{-1}: 3660 (H_2O); 3240 (N-H); 3076, 2955, 2901, 2870 (CH_2, CH_3); 1636 (C=O, amide I); 1478 (C–N), 1390 (N=O), 1500 (H_2O), 1270, 1050, 803, 776 (NO_3^-). λ_{max} = 263 nm.

$[ZnCl_2 \cdot Sk]$ (**7**). Yield is 89% (0.2517 g). Brown crystals. Found, %: C 35.16; H 5.11; N 14.77. Calculated, %: C 35.08; H 5.35; N 14.88. IR, ν_{max}, cm^{-1}: 3375, 3331, 3329, 3260 (N-H); 3079, 2974, 2890 (CH_2, CH_3); 1635 (C=O, amide I); 1505 (amide II), 1446 (C–N). λ_{max} = 235 nm.

Main body

The organic ligand spirocarbon has been synthesised. Its composition and structure have been confirmed by spectral methods. The UV spectrum is characterised by an absorption maximum at λ_{max} = 206 nm (see Fig. 2).

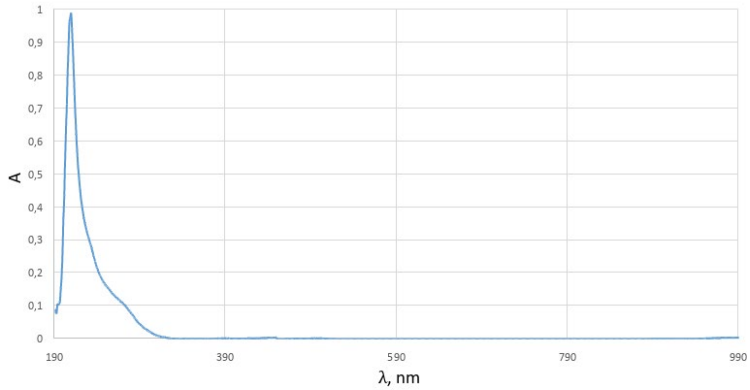

Fig. 2. UV spectrum of spirocarbon

The IR spectrum of compound **1** (see Fig. 3) shows characteristic absorption bands of stretching vibrations corresponding to the functional groups of spirocarbon: carbonyl (1650 cm^{-1}), amino group (3310, 3295, 3203 cm^{-1}), and confirmation of the C-N bond presence (1420 cm^{-1}). The spectral characteristics are consistent with literature data [16].

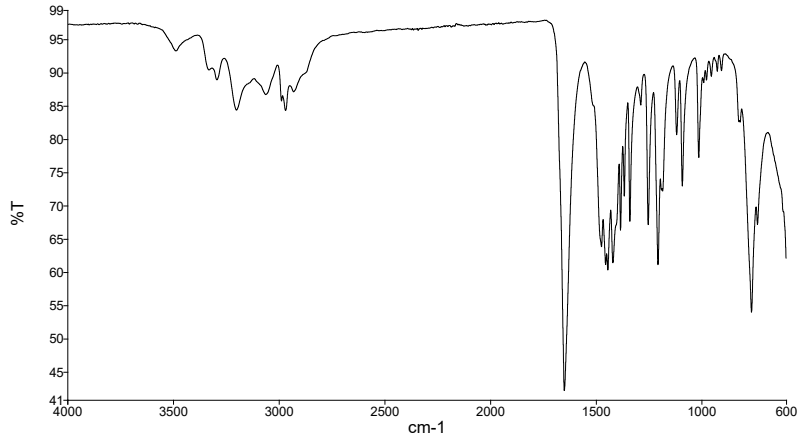

Fig. 3. IR spectrum of spirocarbon

Analysis of spirocarbon complexes IR spectra, the metal is coordinated to the ligand via the oxygen atom of the amide group –CO–NH–. It is evidenced by the shift of the C=O band to the long-wavelength region of the spectrum. This is supported by electronic spectroscopy data: a series of bathochromic shifts corresponding to $\pi \rightarrow \pi^*$ transitions are observed (see Figs. 4 and 5).

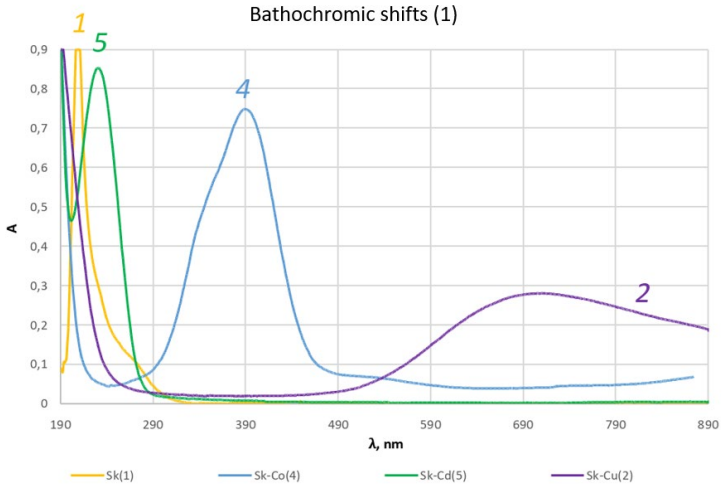

Fig. 4. Electronic spectra of the compounds **1**, **4**, **5**, **2**

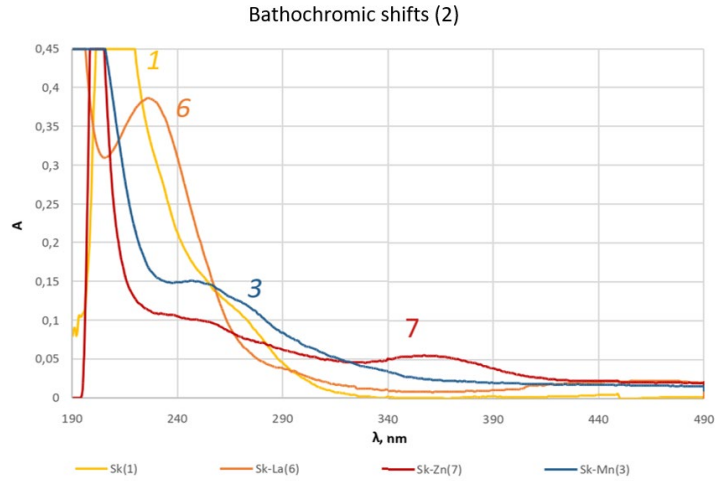

Fig. 5. Electronic spectra of the compounds **1**, **6**, **7**, **3**

Identification of biological targets for spirocarbon was conducted using the PASS Online web service [17]. It forecasts the probability of its interaction with various molecular targets based on the analysis of the compound's molecular structure. Table 2 shows the proteins forecasted as potential direct targets for interaction with the ligand.

Table 2. Forecasting the interaction with molecular targets

Name	Probability of interaction with biological targets
α-Synuclein	0.8237
Serine/threonine-protein kinase PLK3	0.3635
Protein kinase C iota	0.3443
Neuronal acetylcholine receptor subunit alpha-7	0.3227
ADAMTS-4	0.3266

As a result, the program provided a table containing probable molecular targets, sorted in descending order of the Confidence value (the probability of ligand-target interaction). Proteins with Confidence values exceeding the established threshold of 0.7 were considered priority targets. The Alpha-synuclein protein satisfies this condition [18].

To prepare the ligand structure for subsequent docking, geometry optimisation was performed using the Firefly program [19] via the PM3 method. The result of the geometry optimisation (see Fig. 6) of the molecule in *.out format was visualised using the Chemcraft program [20].

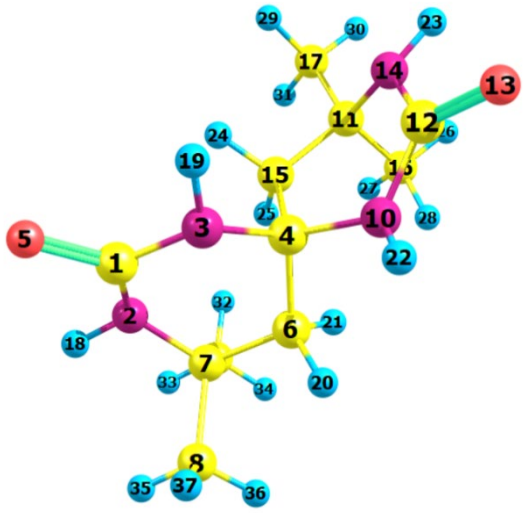

Fig. 6. Optimised geometry of the spirocarbon molecule

Molecular docking was performed to evaluate the mechanism of action of spirocarbon due to the absence or limited number of direct structural analogues among known biologically active compounds. As a result of docking using the SwissDock software [21], several possible conformations were identified, i.e., variants of the spatial arrangement of the ligand in the complex with the protein, differing in binding energy. The most geometrically similar conformations are grouped into clusters; their averaged characteristics are ranked by binding energy (cluster rank). It is shown in Table 3.

Table 3. Energetic characteristics of ligand conformations.

Conformation	Cluster	Rank of cluster	Energy (kcal/mol)
1	0	0	-6.34
2	4	3	-6.27
3	23	0	-6.25
4	12	0	-6.22
5	6	3	-5.91

Conformations with the lowest (most negative) energy values, reflecting the most stable ligand-protein interaction, were selected for further analysis.

Conformation 1

Cluster: 0

ClusterRank: 0

Energy is -6.34 kcal/mol

The following bonds were formed (see Fig. 7):

- The oxygen atom of the amide group of 4,4,10,10-tetramethyl-1,3,7,9-tetraazaspiro[5.5]undecane-2,8-dione.
- The hydrogen atom (HN) of the ASP115/HN, MET116/HN, GLU114/HN groups.
- The hydrogen atom (NH) and MET116/O, GLU`114/HN formed a hydrogen bond.

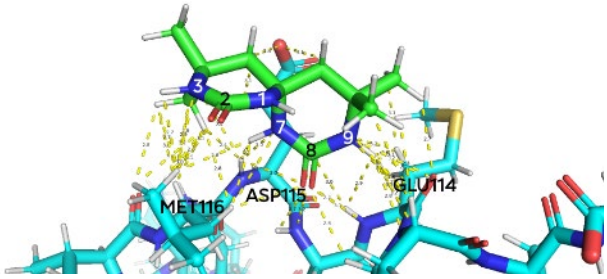

Fig. 7. Formation of a bond between 4,4,10,10-tetramethyl-1,3,7,9-tetraazaspiro[5.5]undecane-2,8-dione and the enzyme's active site (conformation 1)

Conformation 2

Cluster: 4

ClusterRank: 3

Energy is 6.27 kcal/mol

The following bonds were formed (see Fig. 8):

- Dipole-dipole interactions: LYS`21/C=O with C=O of the ligand.
- Dipole-induced dipole: the carbonyl group (C=O) is polar. It can induce a dipole in an adjacent C-H bond. It will lead to weak attractive interactions: THR22/H with C=O of the ligand, LYS21/H with C=O of the ligand.
- A multitude of van der Waals forces (dispersion forces) between C-H…H-C; C-H…N.

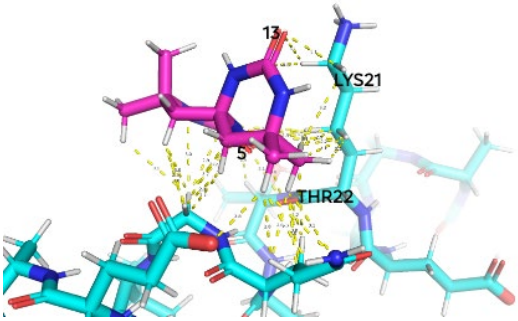

Fig. 8. Formation of a bond between 4,4,10,10-tetramethyl-1,3,7,9-tetraazaspiro[5.5]undecane-2,8-dione and the enzyme's active site (conformation 2)

Conformation 3

Cluster: 23

ClusterRank: 0

Energy is -6.25 kcal/mol

The following bonds were formed (see Fig. 9):

- Hydrogen bonds: LYS96/N-H with C=O of the ligand, LEU100/O with N-H.
- Dipole-induced dipole: the carbonyl group (C=O) is polar. It can induce a dipole in an adjacent C-H bond. This will result in weak attractive interactions: LYS96/H with C=O of the ligand, LYS97/H with C=O of the ligand, LEU`100/H with C=O of the ligand.
- A multitude of van der Waals forces (dispersion forces) between C-H…H-C; C-H…N.

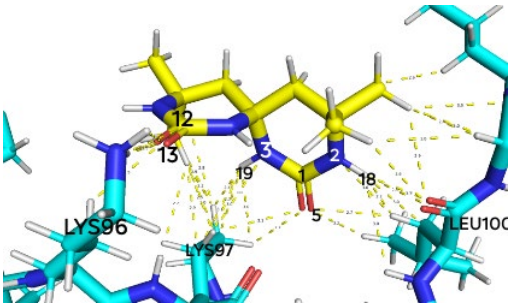

Fig. 9. Formation of a bond between 4,4,10,10-tetramethyl-1,3,7,9-tetraazaspiro[5.5]undecane-2,8-dione and the enzyme's active site (conformation 3)

Conformation 4

Cluster: 12

ClusterRank: 0

Energy is -6.22 kcal/mol

The following bonds were formed (see Fig. 10):

- Hydrogen bonds: LYS`43/O with NH of the ligand.
- A multitude of van der Waals forces (dispersion forces) between C-H…H-C; C-H…N; C-H ... O.
- Dipole-induced dipole: the carbonyl group (C=O) is polar. It can induce a dipole in an adjacent C-H bond. This will result in weak attractive interactions: LYS43/C=O with C-H of the ligand, GLY36/C=O with C-H of the ligand, VAL`40/C=O with C-H of the ligand.

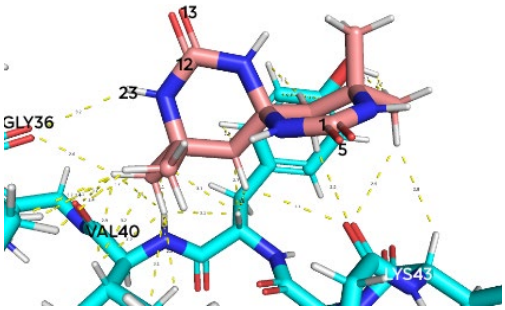

Fig. 10. Formation of a bond between 4,4,10,10-tetramethyl-1,3,7,9-tetraazaspiro[5.5]undecane-2,8-dione and the enzyme's active site (conformation 4)

Conformation 5

Cluster: 6

ClusterRank: 3

Energy is -5.91 kcal/mol

The following bonds were formed (see Fig. 11):

- Hydrogen bonds: LYS58/N-H with C=O of the ligand, GLN62/N-H with N of the ligand.
- A multitude of van der Waals forces (dispersion forces) between C-H…H-C; C-H…N; C-H ... O.

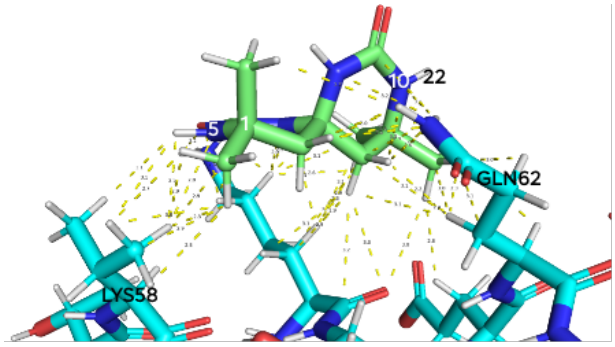

Fig. 11. Formation of a bond between 4,4,10,10-tetramethyl-1,3,7,9-tetraazaspiro[5.5]undecane-2,8-dione and the enzyme's active site (conformation 5)

According to data obtained data on the modes of ligand-target binding, conformation 1 is the most preferred due to being of the zero cluster and possessing the lowest negative binding energy. Similarity in energies is also observed for conformations 1-4 (ΔE_{max} = 0.12 kcal/mol). It may indicate the possible existence of alternative pathways for ligand binding to the target's active site.

To evaluate the drug potential of spirocarbon and its derivatives, lipophilicity was studied using the software package [22] at various pH values to forecast membrane permeability, bioavailability, and pharmacokinetics (see Figs. 12 and 13).

The lipophilicity of spirocarbon (**1**) (Fig. 12, curve 1) shows little dependence on pH. However, in alkaline medium, log D (the compound's distribution coefficient between lipid and aqueous phases; a measure of lipophilicity) decreases sharply due to the presence of a basic –NH group. A lipophilicity value <1 indicates a moderate ability of the free spirocarbon molecule to penetrate cell membranes. The amide group is almost non-ionisable in the pH range of 2-12 and has little effect on log D changes in this range.

In the Cu^{2+} complex (**2**), log D (Fig. 12, curve 2) increases at low pH values up to 7. It occurs due to the gradual deprotonation of a weak basic group, thereby increasing the molecule's lipophilicity. Protonation arises from the presence of a basic –NH group or protonation of water molecules coordinated to the metal. In the pH range from 7 to 12, the basic group is fully deprotonated, and there are no other ionisable groups (the amide group does not ionise in this range and forms hydrogen bonds). Lipophilicity >2 indicates good absorption and bioavailability [23].

The Mn^{2+} complex (**3**) (Fig. 12, curve 3) features a weakly and gradually deprotonating basic –NH group. It increases the molecule's lipophilicity. The value remains constant in the pH range of 6-11. A value of 1.9 shows good absorption and bioavailability, likely due to the absence of coordinated water. This water is hydrophilic (the more water molecules and the stronger the "metal-H_2O" bond, the lower the log D).

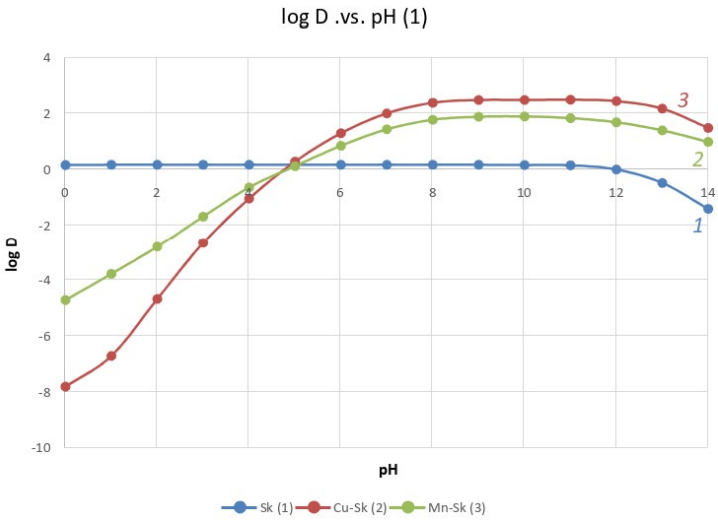

Fig. 12. Plot of log D vs. pH for Sk (**1**), $[CuSk_2(H_2O)](NO_3)_2$, $[ZnCl_2{\cdot}Sk]$

The Co^{2+} complex (**4**) (Fig. 13, curve 4) shows a low increase in log D at low pH values. It is associated with the gradual deprotonation of a weak basic group (-NH or coordinated water). In the pH range of 6-11, lipophilicity increases slightly. At higher pH, lipophilicity <2 indicates moderate absorption and bioavailability (reason: two hydrophilic coordinated water molecules).

The Cd^{2+} complex (**5**) (Fig. 13, curve 5) is characterised by an increase in lipophilicity across the entire pH range of 0-12. It is attributed to the hydrophilicity imparted by coordinated nitrate anions and steric effects that hinder the complex's penetration into lipid environments.

The La^{3+} complex with spirocarbon (**6**) (Fig. 13, curve 6) shows the lowest log D values overall across the pH range of 0-12. It is due to hydrophilicity and steric effects (properties arising from the presence of nitrate anions). A log D <0 indicates poor permeability through cell membranes.

The Zn^{2+} complex with spirocarbon (**7**) (Fig. 13, curve 7) shows a gradual increase in log D from low pH values up to pH 7 due to the presence of a weak basic NH group deprotonating gradually. Consequently, lipophilicity increases. In the pH range of 6-11, lipophilicity remains constant. A lipophilicity value >2 shows good absorption and bioavailability. Such log D values may be associated with the absence of coordinated water, which is hydrophilic.

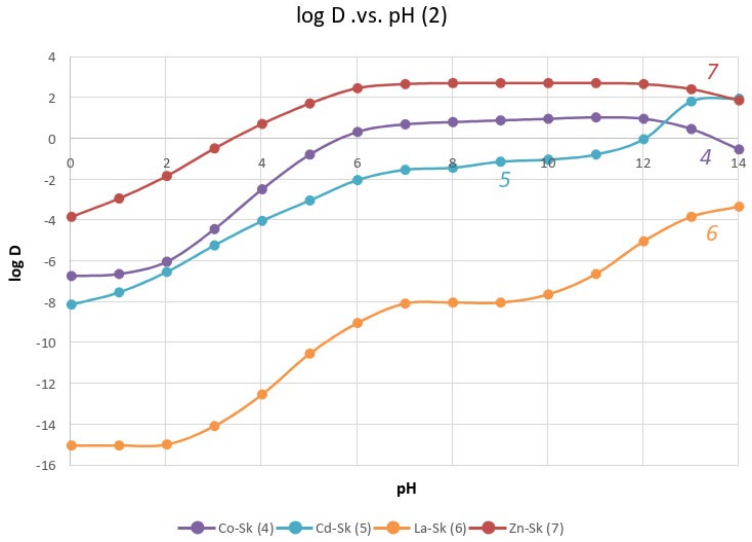

Fig. 13. Plot of log D vs. pH for $[Cd(NO_3)_2Sk(H_2O)]$, $[LaSk_2(H_2O)_2(NO_3)_3]$, $[CoSk(H_2O)]$, $[Cd(NO_3)_2Sk(H_2O)]$

Conclusions

Complex compounds of spirocarbon with Cu^{2+}, Zn^{2+}, Mn^{2+}, Co^{2+}, Cd^{2+}, La^{3+} cations have been synthesised. Analysis of the IR spectra confirmed metal coordination to the ligand via the oxygen atom of the amide group as evidenced by the shift of the C=O band to longer wavelengths. The magnitudes of the shifts were 29 cm^{-1} (Cu^{2+}), 15 cm^{-1} (Zn^{2+}), 5 cm^{-1} (Mn^{2+}), 28 cm^{-1} (Co^{2+}), 32 cm^{-1} (Cd^{2+}), and 14 cm^{-1} (La^{3+}). Absorption maxima are as follows: λ_{max1} = 243 nm; λ_{max2} = 235 nm; λ_{max3} = 269 nm; λ_{max4} = 515 nm, λ_{max5} = 269 nm, λ_{max6} = 263 nm. Based on docking analysis results, the identified biological target - α-synuclein - binds to the ligand (spirocarbon) via hydrogen bonds between the oxygen and hydrogen atoms of the amide group of 4,4,10,10-tetramethyl-1,3,7,9-tetraazaspiro[5.5]undecane-2,8-dione and the hydrogen and oxygen atoms of the amino acid residues of the protein. The lipophilicity study shows good absorption and bioavailability for Zn^{2+} and Mn^{2+} complexes in the pH range of 6-11 (the ligand showed moderate values). The obtained data provide broad prospects for the future biomedical application of spirocarbon and its metal complexes.

Conflict of interest

The authors declare they have no financial or other interests.

References

1. **Weinschenk A.U.** Condensation von Aceton mit Harnstoff. *Ber. Dtsch. Chem. Ges.*, 1901, 34(**2**), 2185-2187.
2. **Zigeuner G., Fuchs E., Brunetti H.** Über Heterocyclen, 8. Mitt.: Über 6,6′-Spirobis-(2-oxo-bzw. 2-thionohexa-hydropyrimidine). *Monatsh. Chem.*, 1966, 97, 36-42. DOI: 10.1007/BF00905481.
3. **Alam M., Ahmad M., Rasheed A., Ahmad A.** Biopharmaceutical studies of spirobishexahydropyrimidine. *Indian J. Exp. Biol.*, 1992, 30(**12**), 1181-1183.
4. **Dudok K.P., Fedorovych A.M., Dudok T.G., Rechytskyi O.N., Yeresko V.A., Shkavoliak A.V., Sibirna N.O.** Influence of spirocarbon and pyrrolopyrimidinedione derivatives on physicochemical characteristics of ligand forms of hemoglobin in vitro. *Studia biologica*, 2009, 3(**2**), 23-34.
5. **Starykovych L.S., Starykovych M.A., Rechytskyi A.N., Yeresko V.A., Kosiak T.Yu., Sibirna N.A.** Study of the influence of spirocarbon and pyrrolopyrimidinedione derivatives on leukemia cells. *Studia biologica*, 2009, 3(**2**), 93-98.

6. **Dudok K.P., Starykovych M.A., Rechytskyi A.N., Shkavoliak A.V., Sibirna N.A.** Role of pyrrolopyrimidinedione derivatives in regulation of physicochemical characteristics of hemoglobin and activity of individual enzymes of antioxidant defense of human blood in vitro. *Visnyk of the Lviv University. Series Biology*, 2012, 60, 126-136.
7. **Musatov A.G., Semyashkina A.A., Dashevskiy R.F.** Factors for optimizing the formation of plant productivity and grain quality of spring barley and oats. *Khranenie i pererabotka zerna [Storage and Processing of Grain]*, 2007, 7, 38-41 (in Russian).
8. **Zlobin A.I.** Morphophysiological and biochemical changes in barley plants under treatment with growth regulators, Cand. Sci. (Biol.) dissertation. Moscow, 1994, 18 p. (In Russian).
9. **Wagner W.J., Gross M.L.** Using mass spectrometry-based methods to understand amyloid formation and inhibition of alpha-synuclein and amyloid beta. *Mass spectrom. rev.*, 2024, 43(**4**), 782-825. DOI: 10.1002/mas.21814.
10. **Li S., Liu, Y., Lu S., Xu J., Liu X., Yang D.** A crazy trio in Parkinson's disease: metabolism alteration, α-synuclein aggregation, and oxidative stress. *Mol. Cell. Biochem.*, 2025, 480(**1**), 139-157. DOI: 10.1007/s11010-024-04985-3.
11. **Zueva I.V., Vasilieva E.A., Gaynanova G.A., Moiseenko A.V., Burtseva A.D.** Can activation of acetylcholinesterase by β-amyloid peptide decrease the effectiveness of cholinesterase inhibitors? *Int. J. Mol. Sci.*, 2023, 24(**22**), 16395. DOI: 10.3390/ijms242216395.
12. **Gajendra K., Pratap G.K., Poornima D.V., Shantaram M., Ranjita G.** Natural acetylcholinesterase inhibitors: a multi-targeted therapeutic potential in Alzheimer's disease *Eur. J. Med. Chem. Rep.*, 2024, 11, 100154. DOI: 10.1016/j.ejmcr.2024.100154.
13. **Mortada S., Karrouchi K., Hamza E.H., Oulmidi A., Bhat M.A., Mamad H.** Synthesis, structural characterizations, in vitro biological evaluation and computational investigations of pyrazole derivatives as potential antidiabetic and antioxidant agents. *Sci. Rep.*, 2024, 14(**1**), 1312. DOI: 10.1038/s41598-024-51290-6.
14. **Hadda T.B., Deniz F.S., Orhan I.E., Zgou H., Rauf A., Mabkhot Y.N., Maalik A.** Spiro heterocyclic compounds as potential anti-alzheimer agents (Part 2): Their metal chelation capacity, POM analyses and DFT studies. *Med. Chem.*, 2021, 17(**8**), 834-843. DOI: 10.2174/1573406416666200610185654.
15. **Shubina A.A., Orlova T.N.** Synthesis and structural features of La(III) complex compounds with organic ligands. *Cifra. Khimiya.* 2024, 1(**1**), 1-13. Available at: https://chemistry.cifra.science/archive/1-1-2024-april/10.18454/CHEM.2024.1.5 (accessed 20.07.2025). (In Russian).
16. **Netreba E.E., Fedorenko A.M., Pavlov A.A.** Synthesis and study of the molecular-crystal structure of 4,4,10,10-tetramethyl-1,3,7,9-tetraazaspiro[5.5]undecane-2,8-dione. *Nauk. visnyk Uzh. univ. Ser.: Khimiya [Scientific Buelletin of Uzhhorod University. Series: Chemistry]*, 2011, 1, 107-116.
17. **Filimonov D.A., Lagunin A.A., Gloriozova T.A., Rudik A.V., Druzhilovskii D.S., Pogodin P.V., Poroikov V.V.** Prediction of the biological activity spectra of organic compounds using the PASS online web resource. *Chem. Heterocycl. Comp.*, 2014, 50(**3**), 444-457. DOI: 10.1007/s10593-014-1496-1.
18. **Ulmer T.S., Bax A., Cole N.B., Nussbaum R.L.** Structure and dynamics of micelle-bound human alpha-synuclein. *J. Biol. Chem.*, 2005, 280(**10**), 9595-9603. DOI: 10.1074/jbc.M411805200.
19. **Granovsky A.A.** Firefly version 7.1.G, Available at: http://classic.chem.msu.su/gran/firefly/index.html (accessed 20.07.2025).
20. **Zhurko G., Zhurko D.** Chemcraft: graphical software for visualization of quantum chemistry computations. Version 1.8 (build 682). Chemcraft website. 2025. Available at: https://www.chemcraftprog.com (accessed: 20.07.2025).
21. **Grosdidier A., Zoete V., Michielin O.** SwissDock, a protein-small molecule docking web service based on EADock DSS. *Nucleic Acids Res.*, 2011, 39 (Web Server issue), 270-277. DOI: 10.1093/nar/gkr366.
22. **ChemAxon** Log D vs. pH Predictor. ChemAxon. Available at: https://chemaxon.com/products/logd-predictor (accessed: 20.07.2025).
23. **Wu K., Kwon S., Zhou X., Fuller C., Wang X., Vadgama J., Wu Y.** Overcoming Challenges in Small-Molecule Drug Bioavailability: A Review of Key Factors and Approaches. *Int. J. Mol. Sci.*, 6, 25(**23**), 13121. DOI: 10.3390/ijms252313121.

Received 23.07.2025
Approved 27.08.2025
Accepted 09.09.2025